

2001

Effect of the sinter-forging deformation rate on properties of Bi-2223 current leads

X. K. Fu

University of Wollongong

Y. C. Guo

University of Wollongong, yanhui@uow.edu.au

W. M. Chen

University of Wollongong

Hua-Kun Liu

University of Wollongong, hua@uow.edu.au

S. X. Dou

University of Wollongong, shi@uow.edu.au

Follow this and additional works at: <https://ro.uow.edu.au/engpapers>



Part of the [Engineering Commons](#)

<https://ro.uow.edu.au/engpapers/8>

Recommended Citation

Fu, X. K.; Guo, Y. C.; Chen, W. M.; Liu, Hua-Kun; and Dou, S. X.: Effect of the sinter-forging deformation rate on properties of Bi-2223 current leads 2001.
<https://ro.uow.edu.au/engpapers/8>

Effect of the sinter-forging deformation rate on properties of Bi-2223 current leads

X. K. Fu, Y. C. Guo, W. M. Chen, H. K. Liu and S. X. Dou

Abstract—The influence of the sinter-forging rate on the critical current density (J_c) behaviour in an external field and on the contact resistance R_c for Bi-2223 current leads has been investigated. The current leads were fabricated by a combination of Cold Isostatic Pressing (CIP) and sinter-forging methods with the thickness reduction rate ranging from 0% to 90%. The two silver contact terminals of each sample were also prepared during the sinter-forging. The results revealed that J_c was strongly affected by the deformation rate of sinter-forging and reached a maximum of 725 A/cm^2 at a deformation rate of 80%. From the measurements of the external magnetic field dependence on J_c , it was determined that sinter-forging could improve the J_c behaviour in external fields, particularly in the regime below 10×10^{-3} Tesla (i.e., 10 mT). The measurements of the contact resistance R_c were conducted for different transport currents at 77 K. The results showed that the contact resistance for the samples with higher deformation rates became less dependent on the transport current over a range of 0.5 A to 50 A.

Index Terms—Current lead, electrical contact, critical current density, high temperature superconductor.

I. INTRODUCTION

Bismuth-2223 is one of the most successful high- T_c superconductors for practical applications, such as current leads in SMES and current limiters [1], [2]. From the technological point of view, there are two important aspects to such current leads: 1. good critical current density performance in external fields, 2. and low contact resistance of the two terminals. Sinter-forging has been widely applied to fabricate small pellets, and critical current densities over 1000 A/cm^2 have been achieved at 77 K [3], [4]. This

method has the potential to be used for fabricating large size bulks for applications such as current leads. On the other hand, CIP is a suitable technique for preparing large size and complicated shaped samples for ceramic powders. In this work, the combination of CIP and sinter-forging was used to fabricate Bi-2223 current leads, and their critical current density and contact resistance performances were investigated.

II. EXPERIMENTAL

The rods are composed primarily of the Bi-2212 phase, but other minor phases such as Bi-2201 and Ca_2PbO_4 are also present. They are prepared by CIP with a stoichiometric ratio given by $\text{Bi/Pb/Sr/Ca/Cu} = 1.72/0.34/1.83/1.97/3.13$ and then sintered at 850°C for 120 hours in air. Pellets cut from the rods were sinter-forged twice at 850°C for 25 hours, and their total thickness reduction rates varied from 0 to 90% by applying different pressures (from 0 MPa to 7 MPa) during the process. The four terminals to be used the measurements were prepared and inserted before the second sinter-forging. The complete processing details have been reported earlier [5]. The final dimensions of the samples were around $0.3 \text{ cm} \times 0.7 \text{ cm} \times 5.5 \text{ cm}$. The field dependence on the transport critical current density J_c -B was measured by the four probe method with a $1 \mu\text{V/cm}$ criterion and with the external applied field both parallel and perpendicular to the broad surface of the samples. The bulk density and the contact resistance were measured by the Archimedes method and the three probe method, respectively.

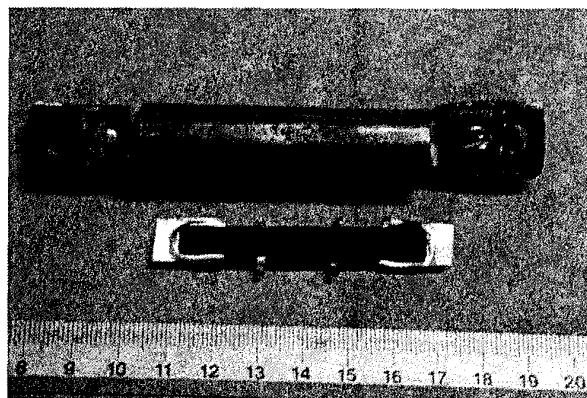


Fig.1 A photo of a sample after sinter-forging (lower) and a prototype (higher) of a current lead.

Manuscript received August 16, 2000. This work was supported by Australian Research Council and Department of Education, Training and Youth Affairs.

X. K. Fu is with the Institute for Superconducting and Electronic Materials, University of Wollongong, NSW 2500, Australia. (telephone: 61-02-4221-5771, e-mail: xf02@uow.edu.au).

Y. C. Guo is with the Institute for Superconducting and Electronic Materials, University of Wollongong, NSW 2500, Australia. (telephone: 61-02-4221-5726, e-mail: ycguo@uow.edu.au).

W. M. Chen is with the Institute for Superconducting and Electronic Materials, University of Wollongong, NSW 2500, Australia. (telephone: 61-02-4221-5798, e-mail: chen@uow.edu.au).

H. K. Liu is with the Institute for Superconducting and Electronic Materials, University of Wollongong, NSW 2500, Australia. (telephone: 61-02-4221-4547, e-mail: hua_liu@uow.edu.au).

S. X. Dou is with Institute for Superconducting and Electronic Materials, University of Wollongong, NSW 2500, Australia (telephone: 61-02-4221-4558, e-mail: shi_dou@uow.edu.au).

TABLE 1
PARAMETERS OF SAMPLES AND THEIR PROPERTIES AT 77 K

Batch No.	Thickness reduction rate (%)	Critical current I_c (A)	Critical current density J_c (A/cm^2)	Mass density (g/cm^3)
1	0	18.7	101	3.8
2	30	33.7	127	4.2
3	60	70.8	309	5
4	80	131	725	5.2
5	90	53	227	5.3

III. RESULTS AND DISCUSSION

Fig.1 is a photograph of a sample after sinter-forging and a prototype of a current lead. The prototype sample was enclosed in a stainless steel tube for protection.

A. Critical current Density Performance

Table 1 lists the critical current densities for samples that have undergone different sinter-forging rates, 0%, 30%, 60%, 70%, 80% and 90%. The values of the critical current and critical current density are the average of the measurements on three samples. The results revealed that the critical current density J_c at 77 K initially increased with the increasing deformation rate, reached the highest value of $725 A/cm^2$ at 80%, and then decreased on further increases in the deformation rate. This indicates that the optimal deformation rate could significantly enhance the critical current density. After post annealing the highest J_c exceeded $1000 A/cm^2$ at 77 K and zero external field [5].

The J_c -B measurements revealed that a proper deformation rate could also improve the critical current density performance in an external field at 77 K. In order to compare the influence of different deformation rates on the critical current density behaviour, the normalised field dependence of critical current density is presented in Fig. 2 for the three samples with deformation rate of 0%, 30% and 80%. For the

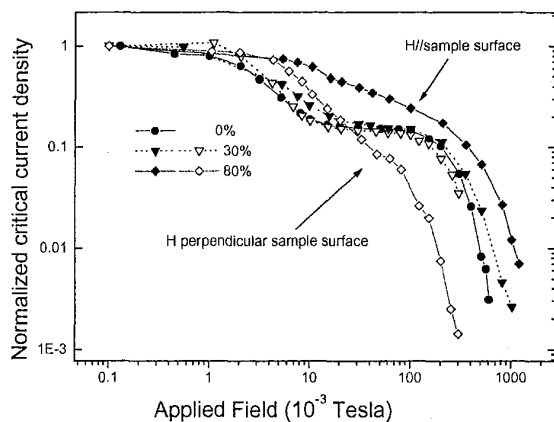


Fig.2 Normalised magnetic dependence of transport J_c at 77 K for three samples with deformation rates 0 %, 30 % and 80 %, respectively.

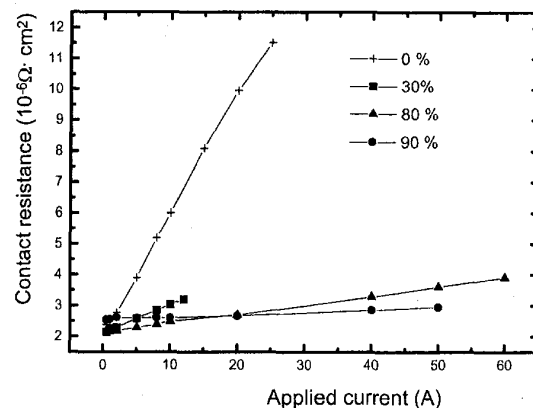


Fig.3 (a) Contact resistance vs transport current at 77 K, measured by the three probe method.

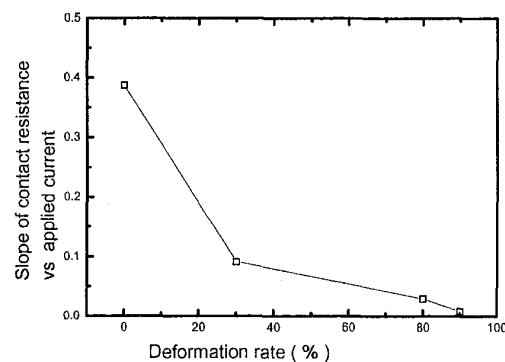


Fig. 3 (b) Ratio of contact resistance and transport current vs deformation rate, calculated from Fig. 3 (a).

sample with 0% deformation rate, J_c -B is not dependent on the direction of the external field because the grains of this sample have no preferred orientation. Moreover the critical current decreases more quickly below 10 mT, compared to the other two samples. On the other hand, there are two curves for each of the other two samples, representing the effect of an external field parallel and perpendicular to the sample's broad surface, as shown in Fig. 2. The critical current for the sample with a deformation rate of 80 % decreases much more slowly than for the other two samples in the region below 10 mT. However, in the region of external field higher than 110 mT, all three samples have the similar tendency to decrease rapidly.

B. Contact Resistance

The contact resistance R_c measurements show that the contact resistances were an order of $10^{-6} \Omega \cdot cm^2$, and for the samples with higher deformation rates, R_c becomes less dependent on the transport current, as shown in Fig. 3 (a) and Fig. 3 (b). Fig. 3 (a) presents the contact resistance R_c as a function of transport current. The results revealed that the

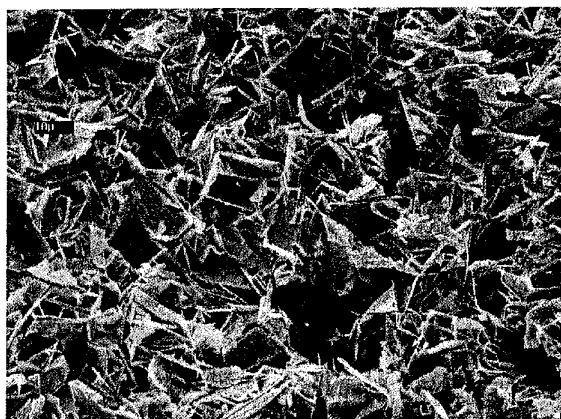


Fig. 4 (a) A SEM image of the fractured cross section for a sample with a deformation rate of 0 %.

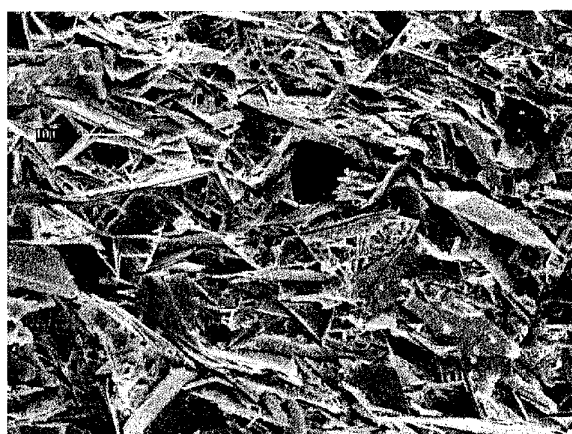


Fig. 4 (b) A SEM image of the fractured cross section for a sample with a deformation rate of 60 %.

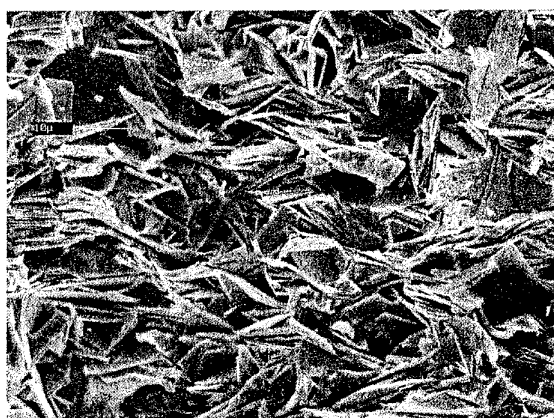


Fig. 4 (c) A SEM image of the fractured cross section for a sample with a deformation rate of 80 %.

contact resistance R_c increases with increasing transport current for all four samples, but it is much less dependent on transport current for higher deformation rates. For example, the sample with a deformation rate of 90% shows very little increase in R_c as transport current increases from 0.5A to 50

A. The ratio between R_c and the transport current is plotted in Fig. 3 (b), and the plot clearly indicates that the value decreases with increasing deformation rate and is nearly zero for the sample with deformation rate of 90 %.

C. Morphology and Microstructure Features

Grain alignment, grain connection and matrix density are the important factors which strongly affect the critical current performance [6]. Three SEM images, Fig.4 (a), Fig. 4 (b) and Fig. 4 (c), show the differences between the three samples with deformation rates of 0 %, 60 % and 80 %, respectively. A higher proportion of irregular grain shapes and grains in poor contact each other appear in Fig. 4 (a). Fig. 4 (b) shows that morphology becomes denser and some grains have a preferred orientation, compared with Fig. 4 (a). However, Fig. 4 (c), shows that the grains in this case form a highly oriented layer structure with plate-like crystals, that the grain contact is better and that the morphology is denser, compared with both Fig. 4 (a) and Fig. (b). This is also supported by the data on mass density presented in Table 1. The mass density normalised by the Bi-2223 theoretical value, 6.2 g/cm^3 , as a function of the deformation rate is plotted in Fig. 5. The plot clearly indicates that the mass density rapidly increases with deformation rate up to 60%, and then increases much more slowly with further increases in deformation rate up to 90 %. On the other hand, too much deformation causes transverse cracks which are harmful to the critical current density performance. For example, some cracks appears on the edges of the sample with a deformation rate of 90%. These positive and negative factors compete each other, so that the sample with deformation rate of 80 % has the best compromise of all these factors. This is the reason why the sample with the deformation rate of 80% has the best critical current density performance, as shown in Fig. 2.

The cross-sectional images show that the samples with higher deformation rates have a better interface between the silver and ceramics. Fig. 6 (a) and Fig. 6 (b) present typical

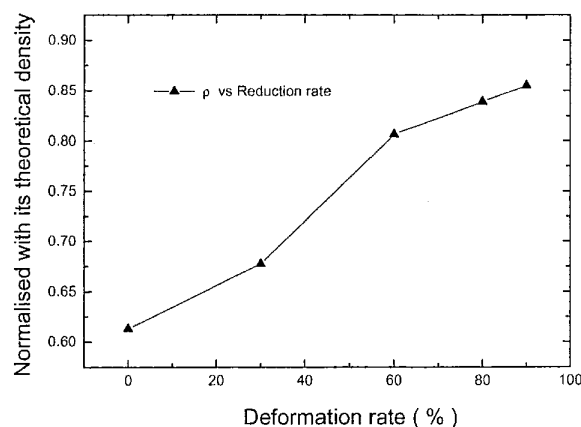


Fig. 5 Density normalised by the Bi-2223 theoretical value (6.2 g/cm^3) as a function of deformation rate.



Fig. 6(a) Cross-sectional image for a sample with a deformation rate of 0 %, the bar in the picture representing 40 μm .



Fig. 6 (b) Cross-sectional image for a sample with a deformation rate of 80 %, the bar in the picture representing 40 μm .

cross-sectional images of samples with deformation rates of 0% and 80%, respectively. The white part and dark part are silver and superconducting ceramics, respectively, and the bar in the picture represents 40 μm . From the two images, it is clearly seen that the sample with a deformation rate of 80 % has a sharper interface between the silver and ceramics. That is why the higher deformation rate improves contact resistances, as shown in Fig. 3 (a) and Fig. 3 (b).

IV. CONCLUSIONS

Bi-2223 current leads were fabricated using a combination of the cold isostatic pressing (CIP) and sinter-forging methods with a thickness reduction rate from 0 % to 90 %. For the samples sinter-forged two times, the critical current density J_c at 77 K reached a maximum of 725 A/cm² for the 80 % deformation sample, and the contact resistances were an order of $10^{-6} \Omega \cdot \text{cm}^2$. Sinter-forging can improve J_c behaviour in the external fields of less than 10 mT. The contact resistance becomes less dependent on the transport current as the deformation increases.

ACKNOWLEDGMENT

X.K Fu thanks T. Silver for her careful proofreading, Dr. J. Horvat for his help in preparing the photograph used in this paper, and is grateful to Australian government and the University of Wollongong providing OPRS and UPA scholarships.

REFERENCES

- [1] R. C. Niemann, Y. S. Cha, J. R. Hull, W. E. Buckles, M. A. Daugherty, B. R. Weber, "High temperature superconducting current leads for micro-SEMS application", IEEE Transactions on Magnetics, vol. 30, n 4 pt 2, July, pp 2589-2592, 1994.
- [2] J. X. Jin, X. K. Fu, H. K. Liu and S. X. Dou, "Bulk Bi-2223 HTS bar strong current performance and applications", unpublished.
- [3] A. Tampieri, G. Celotti, E. Landi G. N. Babini, "Preparation and densification of HTc (2223) phase superconductor" Physica C, vol. 235-240, pt 1, pp 501-502, 1999.
- [4] Norimistu Murayama, Woosuck Shin, "Decomposition of (Bi, Pb)-2223 phase during sinter forging", Physica C, vol. 312, n3-4, pp 255-260, 1999.
- [5] X. K. Fu, V. Rouessac, Y. C. Guo, P. N. Mikheenko, H. K. Liu and S. X. Dou, "Bi-2223 bar current leads fabricated by the combination of cold isostatic pressing and hot pressing" Physica C, vol. 320, pp 183-188, 1999.
- [6] A. Tampieri, D. Fiorani, N. Sparvieri, S. Rinaldi, G. Celotti, R. Bartolucci, "Granular and intergranular properties of hot pressed BSCCO (2223) superconductors" Journal of Materials Science, vol. 34, No. 24, pp 6177-6182, 1999.